A critical review of the preparation, characterization and applications of polyamide membranes

Ayman El-Gendi

Chemical Engineering Department, Engineering Research Institute, National Research Centre, 33 El-Bohouth St, Dokki, Giza, Egypt, Post Code 12622, Tel. +20233335494; Fax: +20233370931, email: aymantaha2010@yahoo.com

ABSTRACT

Polyamide (PA) membranes made by interfacial polymerization (IP) have transformed large-scale desalination and resulted in drinkable inexpensive water being readily available globally to millions of individuals. The enhanced understanding of the extraordinary capabilities exhibited by these polymeric films is critical for further improvement and utilization of the technology. This article critical reviewed PA membrane formation, characterization, and applications. The membranes could be successfully prepared via phase inversion process (PI), interfacial polymerization (IP) and electro-spinning. However, the electro-spinning process was limited by very slow rates of fiber production. Mathematical models have been developed to describe the behavior of PA membrane preparation by the phase inversion process (PI). The effect of polyamide composition on the change of Gibbs free energy was always negative. The mixing of polymer solution was stable for all the polymers compositions at room temperature. PI and IP were the most utilized methods for preparing PA membranes. The PA membrane properties can be characterized by morphology, surface roughness, mechanical and hydrophilic properties, swelling degree, contact angle, membrane charge and gel content, which in turn are dependent on the membrane preparation parameters. The most important characterization methods for PA membrane properties were examined. The applications of PA membranes as pressure driven separation processes were discussed.

Keywords: Polyamide membranes; Formation; Preparation; Characterization; Application; Porous structure; Performance

1. Introduction

Large-scale membrane-based desalination and water reuse have transformed the global water shortage challenge by being able to provide adequate and safe potable water [1]. Nevertheless, water supply requirements for drinking, urban, and industrial applications have remained one of the most significant challenges facing humanity. If a sustainable solution is not found, it will become an even more serious worldwide calamity [2].

Membrane technology is preferred compared to other separation technologies for water treatment due to its low cost, low energy requirement, easy operation and acceptable performance [2]. The state-of-the-art reverse osmosis (RO) and nanofiltration (NF) membranes often adopt a thin-film composite structure [3,4], where a polyamide thin film in thickness of 10–300 nm is in situ generated on top of a porous substrate by an interfacial polymerization (IP) reaction [5,6]. Electrospun polymer nanofibers have been developed as one of the emerging and promising engineered materials for membrane synthesis due to a considerable high porosity, high permeate flux and selectivity, excellent physicochemical stability, and tunable properties.

Usually, membranes may be prepared or fabricated from organic materials such as polymers [7–9] or inorganics such as ceramics [3,4] with polymers being the more common [5,6]. Material selection and membrane pore size depend on the membrane preparation method and application [10]. This will affect the physical and chemical membrane properties of prepared membranes including the ability to retain molecules [11] as well as the driving force required in membrane separation systems [12–16]. Crucial first steps are deciding on a suitable membrane material and a membrane-forming technique or preparation method [17–21] (Table 1). Choice of the membrane raw materials for the required application is dependent on good chemical resistance, permeability, selectivity, and high mechanical strength of the polymer [22–30].

A variety of membrane synthesis or preparation techniques have been developed including phase inversion (PI), interfacial polymerization (IP), track-etching for capillary pore membranes, stretching, sintering, and electro-spinning [12,13]. Phase inversion and interfacial polymerization have been the most employed for symmetric, asymmetric, and thin-film composite (TFC) membranes (Table 1). In addition, the membrane morphology has been assessed [14–17]. Owing to the complexity of membrane preparation parameters, modeling has been found to be useful for predicting the behavior of membrane/ polymer solutions under different conditions. The Flory-Huggins theory [18] for example was created as a suitable framework for thermodynamic examination of membrane preparation factors. Characteristics of membranes applied in water and wastewater treatment market are represented in Table 2.

Polyamides are suitable for preparing most types of membranes such as pervaporation membranes such as: aliphatic polyamide; polyamide-6, polyamide-66, and pressure driven membranes such as TFC PA) as in Table 1 [23–24].

Table 1
Polymeric membrane material and its application via membrane separation process

Polymeric materials	Membrane process	References
Polyamide (PA)	MF, UF, NF, RO, PV	[23,24]
Polyimide (PI)	NF/RO	[3–5,8,9]
Cellulose acetate (CA)	RO	[23]
Polyvinyl chloride (PVC) Polyacrylonitrile (PAN)	NF/RO	[23,24]
Polysulfones (PS) Polyethersulfones (PES) Polyethylene (PE) Polyvinylidene fluoride	UF	[23,24]
Polytetrafluoroethylene (PTFE) Polypropylene (PP) Polyvinylidene fluoride (PVDF)	Membrane distillation	[24]

where MF: microfiltration, UF: ultrafiltration, NF: nanofiltration, RO: reverse osmosis, PV: pervaporation.

This article critical reviewed polyamide membrane preparation, characterization, and applications. The most important characterization methods for polyamide membrane properties were discussed. The applications of polyamide membrane as pressure driven membrane separation processes were examined.

2. Polyamide membrane preparation

The most utilized techniques for polyamide membrane preparation include phase inversion (PI), interfacial polymerization (IP), track etching for capillary pore membranes-microfiltration, stretching, sintering, and electro-spinning [20–22] as shown in Fig. 1a. Previous reports have shown that while the phase inversion process (PI) and interfacial polymerization (IP) are the most common, electro-spinning was limited due to slow rates of fiber production.

2.1. Phase inversion for fabricating polymeric membranes

Duraikkannu et al. [31] in a recent review on a phase inversion (PI) technique-based polymer microsphere fabrication determined that an advantage the PI method was the ability to produce a tailor-made morphology that was a critical factor in separation/ adsorption/ transport systems. They noted that these controlled morphology microspheres were useful storage devices for loading chemical and biological components such as drugs, enzymes, and antioxidants, for environmental pollution control applications. It can be argued that phase inversion (PI), defined as a de-mixing process where an initially homogeneous polymer solution is changed to a solid state [23,24], is a crucial process in sustainable development applications.

The majority PI membranes are fabricated from, polyamide (PA), polyethersulfone (PES), cellulose acetate (CA), polysulfones (PS), cellulose diacetate (CD), polyvinyl chloride (PVC), polyacrylonitrile (PAN), and polyvinylidene fluoride (PVDF). Through the PI process, the composition of the polymer casting solution, pre-concentration time, and immersion bath type it is possible to control the pore size distribution and pore structure of polyamide membranes. Likewise, the phase inversion or separation process can be accomplished in several ways, namely: non-solvent induced phase separation (NIPS), thermally-induced phase separation (TIPS), evaporation-induced phase separation (EIPS) and vapor-induced phase separation (VIPS) [25–28].

2.1.1. Non-solvent induced phase separation

The polyamide membrane may be fabricated by NIPS in a five-step process [29–33]. A polyamide casting solution is prepared by dissolving the polyamide in a suitable solvent. The solution is then casted on a suitable support such as glass by using doctor blade or film applicator. The cast films are subsequently immersed in an immersion bath containing a non-solvent such as water. The films are then taken from the coagulation bath for drying and then storing until characterization. Generally, this technique is used for preparing asymmetric membranes such as reverse osmosis (RO), nanofiltration (NF), and ultrafiltration (UF). While the track-etching method is employed

Table 2
Characteristics of membrane products applied in water treatment market [19]

Membrane	Membrane material	Nominal separation rang	Applications
SR100	Polyamide	200 MWCO	Organics reduction, sulfate removal
TFC®-S	Polyamide	80%–90% NaCl rejection	Water softening, wastewater polishing
TFC-HR	Polyamide	99.55% NaCl rejection	Pure water, brackish water desalination, polishing of industrial wastewater UF permeate
TFC-FR	Polyamide	99.55% NaCl rejection	Fouling resistant membrane for brackish water desalination, polishing of industrial wastewater UF permeate
TFC-XR	Polyamide	99.75% NaCl rejection	Brackish water desalination, polishing of industrial wastewater UF permeate
TFC-SW	Polyamide	99.75% NaCl rejection	Seawater desalination
TFC-HF	Polyamide	99.75% NaCl rejection	Seawater desalination, high flow
HFP-707	PVDF	120,000 MWCO	Oily wastewater treatment
HFK-131	PES	10,000 MWCO	Industrial water treatment

where PVDF: Polyvinylidene fluoride, PES: Polyethersulfone.

for membranes with a symmetric structure. A schematic of the immersion precipitation method is shown in Fig. 1b.

2.1.2. Evaporation, vapor, and thermally induced phase separations

Polyamide membranes may be fabricated using EIPS. A polyamide solution is cast on a porous support fixed on a substrate such as glass or Teflon and then. The cast polyamide solution is exposed to an atmosphere so that the solvent evaporates resulting in a thin polyamide sheet on a porous support. In the case of VIPS, phase inversion of the polyamide solution occurs because of the presence of a non-solvent such as water vapour, which penetrates the polymer solution causing demixing/precipitation [27,28]. The TIPS is dependent on the fact that the solvent feature generally decreased once the temperature is decreased. Subsequent, the demixing is occurred [28–30].

2.2. Interfacial polymerization and continuous membrane formation

Interfacial polymerization (IP) is another common process for membrane formation [34–39] being employed for thin-film composite (TFC) membranes [40–43]. Polyamide TFC have been applied in both NF and RO separation techniques for water desalination [44,45]. TFCs are normally prepared from a reaction of two different monomers on the surface of a microporous support such as polyethersulfone [46–49]. The top surface of the TFC membranes is nonporous and very thin to allow for controlled permeability and selectivity [48–54]. Researchers have reported on polyamide TFC membranes and noted that the type of the monomers selected for the interfacial polymerization is crucial [55–62]. This includes aromatic polyamide membranes [63–71]. An example of a continuous process for fabricating TFC membranes is shown in Fig. 2. Good reviews can be found in the literature [1,69–71].

The asymmetric polyamide TFC polyamide membranes consist of a nonwoven fabric layer, a porous substrate layer

and very dense thin polyamide layer (Fig. 3). A review of the literature indicates that the most utilized porous substrates were prepared from polyethersulfone (PES), polysulfone (PS) or polytetrafluoroethylene (PTFE) by a wet phase inversion process. Usually, the m-phenylenediamine (MPD) and trimesoyl chloride (TMC) are the active monomers used to form the functional polyamide thin dense layer. The preparation of TFC polyamide membranes is depending also on different types of monomers such as: N-N′-diaminopiperazine (DAP), p-phenylenediamine, polyethylenimine, triethylenetetramine (TET), N-(2-aminoethyl)piperazine, and piperazine (PDP) [72–74].

TFC polyamide membranes [32–35] have been employed for NF and RO applications. The TFC membrane is consists of three layers; a thin polyamide layer (<200 nm) created on top of a polyethersulfone (PES) or polysulfone (PS) porous layer (about 50 microns) which is located on top of a non-woven fabric support layer as shown in Fig. 3. This physical arrangement of TFC layers is important to give the best efficiency and to provide mechanical strength. The polyamide top skin layer is responsible for the separation factor (rejection/selectivity) [36]. Detailed studies on poly(tetrafluoroethylene)/ polyamide thin-film composite membranes via interfacial polymerization for pervaporation dehydration on an isopropanol aqueous solution polytetrafluoroethylene/polyamide (PTFE/PA) membranes have been reported [34].

2.2.1. Factors affecting thin-film composite polyamide membrane formation and performance

Thin-film composite (TFC) polyamide (PA) membrane formation via interfacial polymerization (IP) reaction is dependent on the synthesis parameters such as reaction time, and monomer type and concentration [37,38]. Researchers have investigated the type of microporous support, the time lag and reaction time, the curing temperature, the type and concentration of monomers, and various solvents and additives [39–41]. Fathizadeh et al. [42] examined the effect of time lag on polyamide membrane formation with different hydrophilic sub layers. They found that the
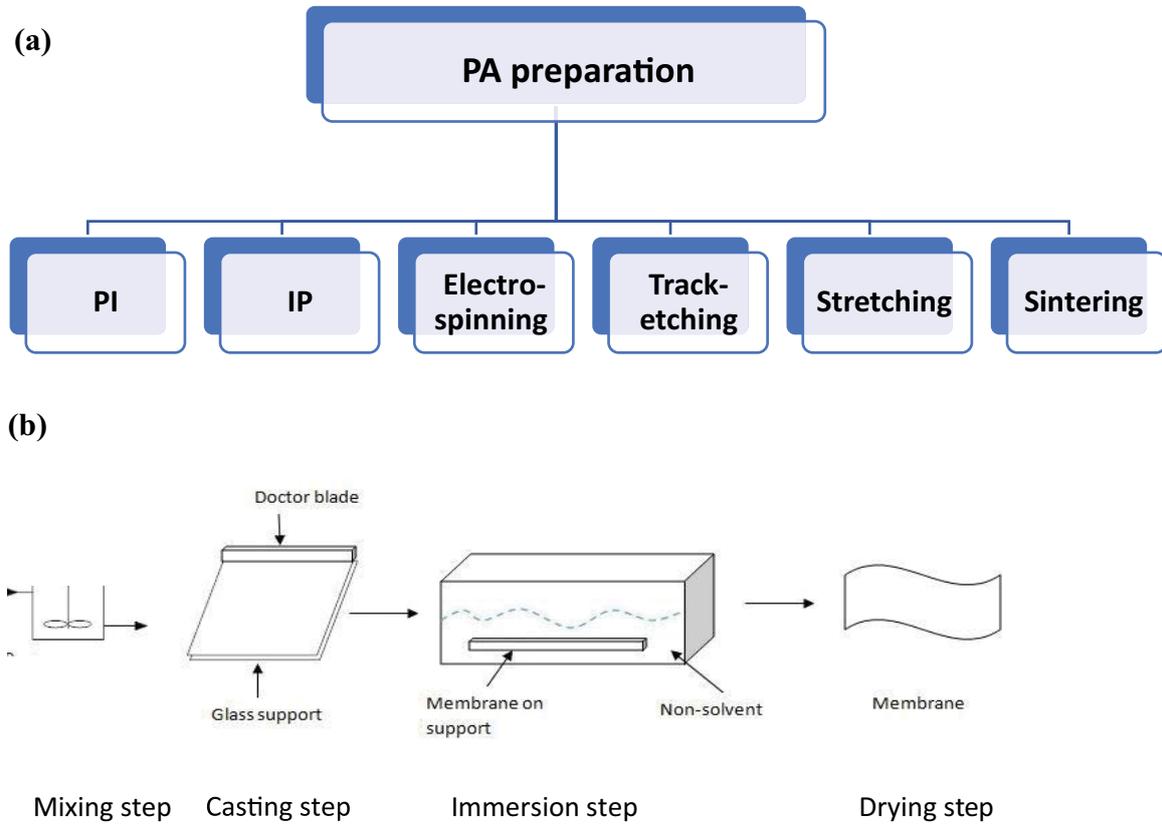
(a)

(b)

Fig. 1. (a) Polyamide membrane preparation techniques and (b) schematic presentation of NIPS process [23–28].
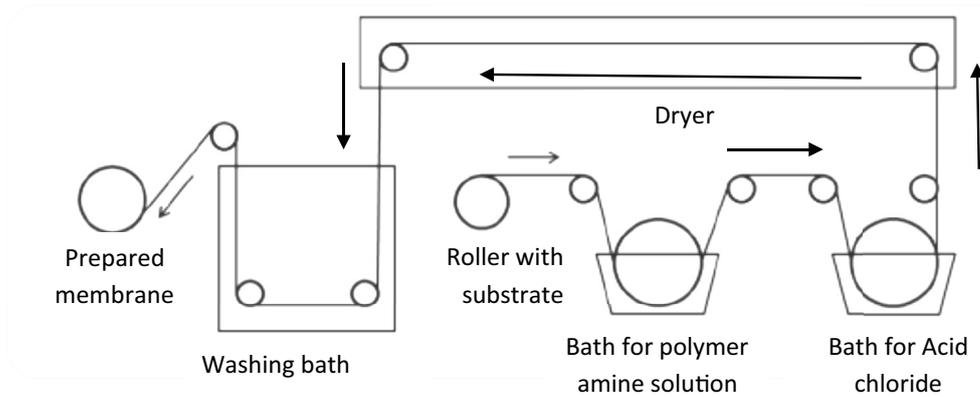

Fig. 2. Schematic diagram of the continuous TFC set-up [8,29].

lag time affected the surface properties of the membranes. Ghosh et al. [20] reported that the reaction time and curing temperature played an important role in cross-linking of the polyamide layer. Some researchers [39–43] described the effects of surface modification on performance properties of polyamide reverse osmosis membranes. They found that the monomer concentration, type of solvent and additives all played an important role in the solubility and diffusivity of the amine and acid monomers in the liquid–liquid interface reaction zone by altering the reaction rate [43]. In a related study, Liu et al., [44] reported that increasing the reaction time led to a reduced membrane permeate flux and an improved salt rejection. Klaysom et al. [45] reported that the water flux increased with a decrease in reaction time, while the performance of the membrane was not dependent on the 1,3,5-benzenetricarbonyl trichloride (TMC, 98%), concentration.

2.3. Modeling of polyamide membrane formation

Polyamide membranes formation relies on the phase inversion process parameters [46]. The composition of the desired or optimum membranes has been determined by experimental work that generally needs time
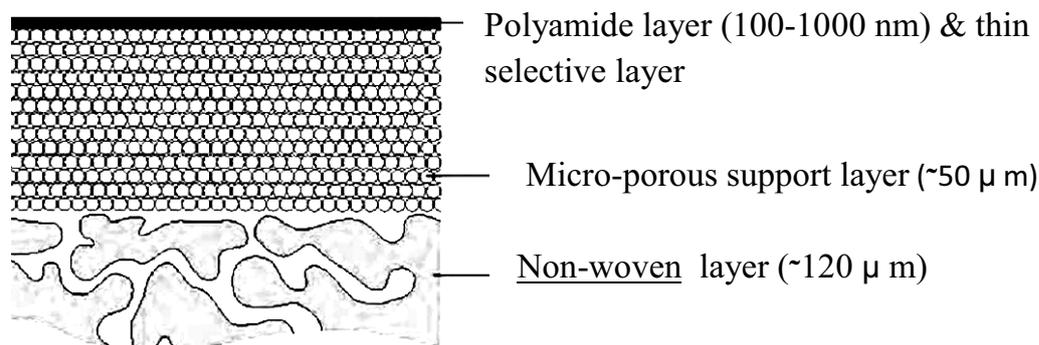
Fig. 3. Schematic diagram of the asymmetric polyamide TFC membrane adapted from [8,33].

for trial-and-error experimentation and raw materials. Mathematical models may be utilized help optimize membrane composition and the manufacturing process. Precise and dependable mathematical models can aid in understanding and controlling membrane formation process and morphology [23].

The Flory-Huggins theory [18] was created to be a suitable and valuable framework for the thermodynamic investigation of membrane formation. The phase inversion procedure can be described as a de-mixing process whereby the initially homogeneous polymer solution is changed in a controlled manner from a liquid state to a solid state [28]. Also, researchers developed mathematical models which depended on varying the volume fraction of each polymer with the volume fraction of solvent over a wide range of conditions [47–49].

The mixing step is the first step in polyamide membrane formation during this step the polyamide is dissolved in a suitable solvent and may be with addition additives or other polymers. The Gibbs free energy of mixing step and chemical potential of each component has been determined for polyamide membranes [48,49]. The literature results showed that the changes in Gibbs free energy of mixing and the chemical potential were always negative. The polymers blend was associated with a negative value of the change of free energy of mixing, $\Delta G_m \approx \Delta H_m \leq 0$ within the phase stability condition ($\delta^2 \Delta G_m / \delta^2 \phi) > 0$, indicating that the miscibility is not limited to two minimum compositions [49]. Therefore, phase separation should not occur during mixing of polymers such as polyamide-6/chitosan (PA-6/CS) [50] and polyamide-6/cellulose acetate (PA-6/CA) [51] over all compositions.

The immersion stage is the second step in polyamide membrane formation by phase inversion. The immersion/precipitation time in the soaking bath is related to the solvent dissolution from polymer solution to the coagulation bath as reported in previous studies [49,50]. A solution with a high polymer concentration forms better membranes [49–57]. Mathematical modelling results suggested that the ratio of polymer solution volume fraction decreased while solvent volume fraction increased with coagulation time due to removal of the solvents from the polymeric solution to the bath. The thickness of polymer on the coagulation plate decreased with time due to solvent removal [50–51]. Mathematical modelling has resulted in a better understanding of the behavior of polyamide membrane formation by phase inversion [50–51]. For example, the effects of polyamide composition on the change of Gibbs free energy were always negative. The mixing was stable for all the polymers compositions at room temperature. A diffusion model allowed for a better understanding of the effect of immersion/precipitation time in the coagulation bath on the polymer blend formation [49–51].

2.4. Optimization of polyamide membrane formation

Polyamide membrane preparation or formation is highly influenced by factors such as casting tool type, velocity of casting, time of casting, pre-concentration time, variation in retention time under water and water temperature variation. Controlling these factors in is difficult especially at the large scale in pilot systems. Based on then literature, the optimum operating conditions for polyamide membrane formation via immersion precipitation (i.e., wet phase inversion) is summarized in Table 3. For example, the optimum immersion step was 1 h at 7°C–25°C. The challenge now is the need for a continuous membrane preparation or production system at the pilot scale. The system should be capable of digitally controlling the drawing speeds in the required range as well as controlling water temperature in the range 7°C–25°C.

3. Polyamide membrane characterization

3.1. Scanning electron microscopy

Generally, membrane properties such as morphology, surface roughness, mechanical strength, hydrophilicity, swelling, and contact angle have an effect on membrane performance [51–55]. The scanning electron microscopy (SEM) [52] has many advantages over traditional microscopes. SEM directly provides the visual information of the top and bottom surface as well as cross-sectional morphology of the polyamide membrane [53–60].

The porosity of the bottom layer occurred by liquid-liquid phase separation while the formation of pores may be attributed to nucleation and growth of the dilute polymer phase [53–55]. In addition, the top layer (active skin layer) is formed by gelation while liquid-liquid phase separation forms the sublayer of the membrane [56–65]. The prepared

Table 3
Optimum operating condition for polyamide membranes prepared by wet phase inversion [44–51]

Membrane preparation step	Optimum operating conditions
Mixing step	Room temperature
Casting speed	10 to 300 mm/s
Pre-concentration step	30–60 s
Casting step velocity	100 cm/min
Immersion step	1 h at 7°C–25°C
Drying step	Depends on membrane application

polyamide membrane could be highly porous or mostly non-porous (dense) as in Fig. 4a.

Rahimpour et al. [61] studied the preparation of thin-film composite (TFC) polyamide nanofiltration (PANF) membranes for water softening and reported the SEM micrographs of the cross-section, top surface, and the top skin layer of the PES support membrane and TFC PANF membrane. The SEM of TFC PANF membrane surface showed that the polyamide layer [(interfacial polymerization of 1,3-phenylenediamine (PDA) with trimesoyl chloride] was formed on the surface of PES substrate. Likewise, Li et al. [62] synthesized a positively charged PANF hollow fiber membrane by the IP of 1,4-bis(3-aminopropyl) piperazine (DAPP) and trimesoyl chloride on the polyacrylonitrile (PAN) ultrafiltration hollow fiber membrane for lithium and magnesium separation. SEM examination of the surface and cross-section of the PAN membranes was done before and after IP. The surface SEM images showed that the membrane surface of PAN membranes before IP was smooth, whereas the surface of membrane after IP was much rougher. In the cross-sectional micrographs, a dense active layer with 100 nm was formed on the top of PAN support membrane after IP.

SEM assist researchers to classify membranes [59–61]. Also, SEM helps researchers to control the membrane morphology, to prove layers formation, and to control membrane thickness [60–65]. El-Gendi et al. [65] reported the effect of addition non-solvent as water on preparation of polyamide-6 membranes with helping of SEM. They reported that the polyamide-6 membranes displayed sponge like and highly porous structures as a consequence of addition water from 5% to 10%.

3.2. Fourier-transform infrared spectroscopy

Fourier-transform infrared spectroscopy (FTIR) has been recognized as a successful technique for examining and differentiating a materials' functional groups, structures of polymers, and their characterizing as reported in previous studies [63–65]. For example, polyamide scans are distinctly different from polycarbonate [63–65]. Furthermore, the effects of APTEOS content and electron beam irradiation on physical and separation properties of hybrid nylon-66 membranes has been reported by Linggawati et al. [64]. Based on the FTIR data, it was reported that irradiated hybrid nylon membranes exhibited the peak characteristics of nylon-66, namely 3,295 cm^{-1} (NH stretching) and 1,630 cm^{-1} (C–O stretching and NH stretching vibration in amide I).

The band at 1,530 cm^{-1} indicated the NH deformation and CN stretching in amide II.

El-Gendi et al. [65] described the FTIR spectrum of polyamide-6 (PA-6) membranes. The spectrum displayed the characteristic bands of PA-6 at 3,312 cm^{-1} (H-bonded N–H stretch vibration), 1,665 cm^{-1} (amide I, C–O stretch), and 1,562 cm^{-1} (amide II, C–N stretch and CO–N–H bend). The peak of 1,668 cm^{-1} (amide I) was detected for the PA-6/water) which was ascribed to the amino groups of PA-6/water membrane.

3.3. Mechanical properties of polyamide membranes

The mechanical properties of polyamide membranes can be varied considerably allowing for wide capabilities in technology [34,47]. The mechanical properties for polyamide membranes have been reported including stress, strain, Young's modules, and the elongation at break [63–68]. Table 4 summarizes the mechanical properties for polyamide membranes in some of pervious works [34,47].

3.4. Determination of polyamide membrane porosity and swelling

Usually, porosity and swelling determination of polyamide membrane is an imperative task to clarify its performance [45,65]. Furthermore, porosity is a significant characteristic for effective membrane separation. El-Gendi et al. [65] reported on the porosity and swelling of polyamide-6 membranes by immersing polyamide samples in water then weighing (W_w). Then, the polyamide membranes were dried and weighed (W_d). The porosity of polyamide membrane was determined from Eq. (1):

$$P_{PA}(\%) = 10,000 \times \left[\frac{(W_w - W_d)}{V} \right] \qquad (1)$$

where P_{PA} is the polyamide membrane porosity; W_w and W_d are the weights of wet and dry membranes (g), respectively; $V = A \times t$ where A is the membrane surface area (cm^2) and t is the membrane thickness (cm).

The swelling ratio (S) of the membranes was calculated according to Eq. (2):

$$S\% = \left\{ \frac{(W_{wet} - W_{dry})}{(W_{dry})} \right\} \times 100 \qquad (2)$$

(a)

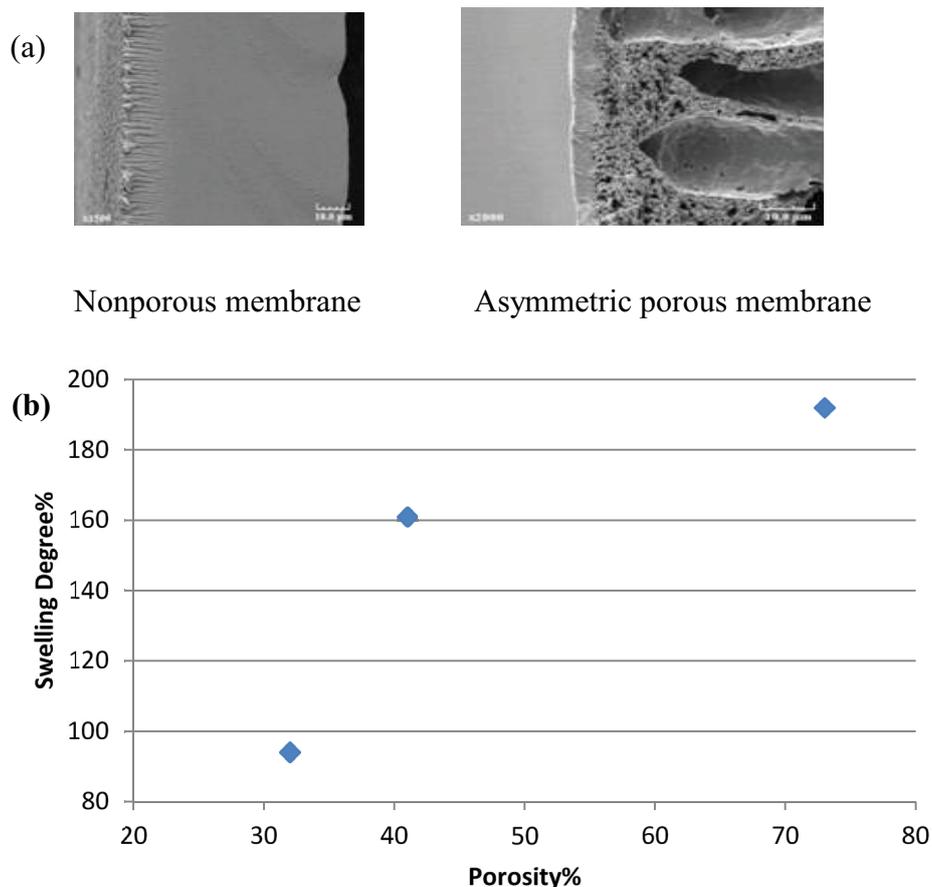Nonporous membrane   Asymmetric porous membrane

(b)

Fig. 4. (a) Cross-section of prepared membranes and (b) effect of membrane porosity on membrane swelling degree [65].

Table 4
Mechanical properties for polyamide membranes

Membrane	Tensile strength	References
Hydrophilic nylon 6,6 nanofibers	10 MPa	[34]
Polyamide-6/cellulose acetate (PA-6/CA)	556.291 (kg/cm^2)	[47]
Nylon 6,6	18 MPa	[64]
Nylon-66	1.8–5.4 (N/mm^2)	[66]

where W_{wet} and W_{dry} are the weight of wet and dry membrane, respectively. This test is important to give an induction of the hydrophilic property of the PA membrane.

El-Gendi et al. [65] reported that the porosity of three types of polyamide-6 membranes was on average 41%–73% (Fig. 4b). Furthermore, the effect of PA membrane porosity on swelling degree is shown in Fig. 4b is in average of 94%–192%. The degree of swelling increased with increasing membrane porosity. As shown in Fig. 4b, the results confirmed that the polyamide-6 membrane swelled to a higher degree, because of the hydrophilic nature of –NH$_2$ which can offer considerable hydrogen bonding with hydrophilic groups (NH$_2$ functional groups act as adsorption sites throughout the membrane)[65]. Similarly, Jadav and Singh [69] studied the preparation of PA nanocomposite

(NC) membranes by IP by incorporating silica nanoparticles. Thicker PA NC membranes formed with higher content of silica. In addition, PA NC membranes had relatively larger pore sizes and pore density. Regarding to the silica load, the pore radii of membrane was in average from 0.34 to 0.73 nm.

Košutić et al. [70] determined the porosity parameters of commercial PA TFC membranes. The authors concluded that the examined PA membranes had different performances, owing to different skin porosities. Also, the porosity and subsequently the performance of the PA membranes changed with operating pressure variation. This was ascribed to more voids that opened at higher pressures. This caused formation of active pores. Kolev and Freger [71] also prepared aromatic PA membranes for

water treatment by RO. They reported that the mass hydration and PA membrane porosity improved over that which could be previously achieved.

3.5. Polyamide membrane performance

Klaysom et al. [45] reported on polyamide/polyacrylonitrile (PA/PAN) thin-film composite osmosis membranes. They examined film optimization, characterization and performance evaluation by assessing pressure, flow rate, and the performance (flux, separation) of different kinds of polyamide membranes (Fig. 5). The permeate water flux (F) was determined from Eq. (3):

$$F = \left(\frac{m}{a} \times t \right) \tag{3}$$

where m: permeate mass in kg, a: membrane active area in m², t: time in hour.

The rejection (R%) percentage was calculated as follows (Eq. 4):

$$R\% = \left(C_f - C_p \right) \times 100 / C_f \tag{4}$$

where C_f: the concentration of the feed solution, C_p: the concentration of the permeate.

4. Polyamide membrane applications

A comprehensive review on the separation performances of polyamide membranes for different applications using reverse osmosis (RO) and nanofiltration (NF) will be provided.

(1) Feeding tank
(2) pump
(3) Pressure gauge
(4) valve
(5) Membrane housing unit
(6) Pressure gauge
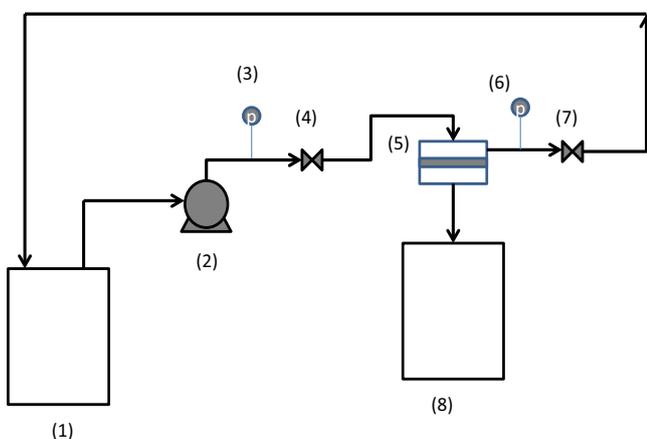**(7) Valve**
(8) Water Permeate

Fig. 5. Schematic diagram of a performance test unit (45).

4.1. Application of polyamide reverse osmosis (PA/RO) membranes

Polyamide (PA) membranes have been applied in numerous separation technologies [64–71] via pressure driven membrane separation techniques such as microfiltration (MF), ultrafiltration (UF), nanofiltration (NF), and reverse osmosis (RO). Typical applications of polyamide membrane in selected membrane processes are summarized in Table 5.

Reverse osmosis (RO) is a well-developed technique that has been widely used for water desalination and water purification/treatment [65–72]. RO membranes are made from cellulose acetate (CA) as an integrally skinned asymmetric semi-permeable membrane via wet phase inversion process for water desalination [29–33]. In the recent decades, RO membranes have been based on a composite material such as TFC polyamide [1–9]. Usually, polyamide reverse osmosis (PA/RO) membranes are considered as dependable and affordable to produce high-quality water with a high productivity through desalination [1–7]. Additionally, using PA/RO membranes appears to be a promising separation tool in the chemical industry [74,75]. The rejection characteristics and permeation of solutions such as seawater, ground water through PA/RO membranes has been reported to be crucial factors [73–76].

Zhang et al. [73] prepared TFC polyamide reverse osmosis (PA/RO) membranes by interfacial polymerization (IP), and reported that the membrane separation performance had a salt rejection of 99% and a permeate flux of 50 kg/m² h at operating condition 32,800 mg/L NaCl aqueous solution as feed at 5.5 MPa and 25°C. Furthermore, Li et al. [74] fabricated semi-aromatic polyamide (SAP)/spherical mesoporous silica nanocomposite reverse osmosis membranes (MSS/RO) membranes using IP. In their studies the membrane separation performance had a salt rejection up to 94%–96% and a permeate flux of 63–73 (kg/m² h) at operating condition 2,000 mg/L NaCl aqueous solution, 25°C, and 1.5 MPa operating pressure. Similarly, Wang et al. [76] fabricated PA/RO membranes via IP. They also found the salt rejection reached to 98%–99% and with a permeate flux of 22–54 kg/m² h. Table 6 summarizes the characterization of the performances of PA/RO membranes [73–76].

4.2. Application of polyamide nanofiltration (PA/NF) membranes

Nanofiltration (NF) has been employed for water treatment, as well as decreasing sludge production [77–81]. Tang et al. [77] reported on the preparation of commercial PA/NF membranes (SWC4, XLE, LE, ESPA3, NE90 and NF90) membranes by interfacial polymerization (IP). Membrane separation performance such as salt rejection reached 90%–97% and permeate flux 54–63 kg/m² h. Moreover, Nilsson et al. [78] assessed the performance of commercial thin-film composite NF PA membranes (NFT-50, NF200, NF90 and Desal-5DK) also prepared using IP. Their membrane separation performance such as salt rejection reached was not quite as good as that of other studies at 40%–95% and permeate flux 53 kg/m² h at operating condition with a

Table 5
Typical applications of polyamide membrane processes [21–27]

Membrane material	Membrane process							
	MF	UF	NF	RO	PV	FO	GS	MD
Aromatic polyamide	√	√	√	√		√		
Aliphatic polyamide	√	√	√	√	√	√		

where, MD: membrane distillation, GS: gas separation, FO: forward osmosis.

feed solution of KCl (20 mM), 60°C at 6 bar. In a related investigation David et al. [79] found much better results with the performance of commercial NF200 membrane (Dow FILMTEC) membranes having a salt rejection of up to 97% and permeate flux 71 kg/m² h with an aqueous feed (MgSO₄). Separation performances of polyamide nanofiltration (PA/NF) membranes are summarized in Table 7.

4.3. Most significant parameters effecting PA membrane performance

Significant factors or parameters affecting membrane performance are shown in Fig. 6.

4.3.1. Effect of operating pressure and temperature on polyamide membrane performance

An increase in operating pressure leads to increasing permeate flux and rejection as demonstrated by Ghosh et al. [82]. Many studies have shown that membrane performance is dependent on the membrane processing technology (MF, UF, NF, RO) [83], including membrane morphology, feed concentration and type of the tested solution. Gherasim et al. [81] for example, studied the performance of a TFC PA/NF membrane (AFC80) in the separation of highly polluting and toxic Pb(II) ions from single salt and binary aqueous solutions simulating real wastewater. They observed that the permeate flux and rejection of lead ions increased with increasing of operating pressure. The authors went on to report that the membrane became positively charged in lead nitrate solution. This behavior was attributed to adsorption of lead ions on the membrane surface. The membrane characteristics thus determined were correlated with the results of lead separation experiments and with the Spiegler–Kedem model parameters.

Polyamide membrane performance is depending on operating temperature of process because of temperature-dependent changes in the polyamide membrane morphology, as well as temperature effects that may be directly or indirectly associated to the decrease in viscosity. Nilsson et al. [78] prepared NF/RO polyamide membranes and reported that a decrease in permeate flux and an increase in potassium chloride rejection as the operating temperature was decreased from 60°C to 20°C and reported also that the effect of NaCl on mass transfer in PA/NF membrane at superior temperatures which have an influence on salt rejection related to temperature effects on mass transfer, that may be directly or indirectly associated with a decrease in viscosity at higher temperature. In a later study, the influence of temperature on the filtration properties of NF membranes was assessed by Manttari et al. [84]. They showed that the membrane permeability decreased at high temperatures in various NF membranes. They attributed this decrease to a reduction in membrane porosity that led to increased membrane separation efficiency and decreased permeate flux. This is an example of temperature-dependent changes in the polyamide membrane morphology, that may be directly or indirectly associated with a decrease in viscosity.

4.3.2. Influence of thermal treatment temperature on polyamide membrane performance

Generally, in pressure driven polyamide membrane separation processes the permeate flux is decreased with increasing thermal treatment temperature of the membranes, whereas the separation factor (membrane selectivity) is increased (such as salt rejection in case of desalination) [25–28]. This may be attributed to that the higher of thermal treatment temperature for the polyamide membrane. The denser of the active polyamide membrane layer and the closer of the pore distribution due to densification of polyamide
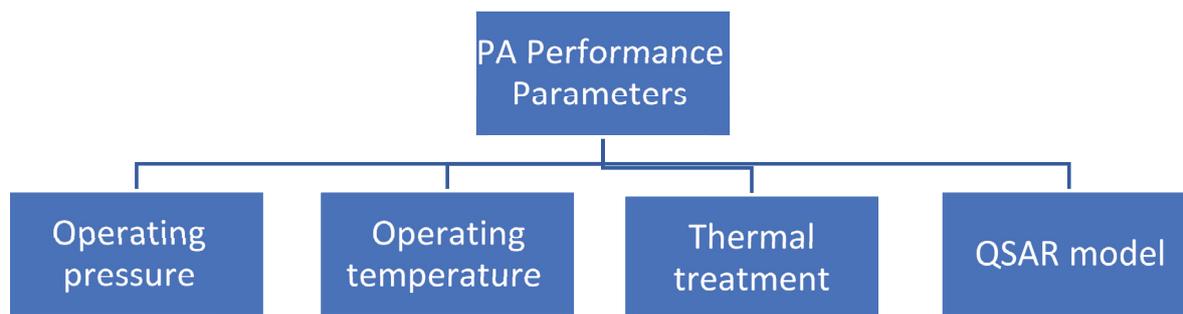

Fig. 6. Polyamide membrane performance parameters.

Table 6
Separation performances of PA/RO membranes

Membrane type	Preparation process	Characterization methods	Permeate flux (kg/m² h)	Salt rejection (%)	Operating condition	References
TFC polyamide reverse osmosis (PA/RO) membranes	Interfacial polymerization (IP)	Attenuated total reflection-infrared (ATR-IR), Swelling Ratio Test, Gel Content Test	50	99	32,800 mg/L NaCl aqueous solution as feed at 5.5 MPa and 25°C.	[73]
Poly(vinyl alcohol) (PVA)/ PA RO) membrane	Poly(vinyl alcohol) coating on (PA RO)		10–52	98–99.5		
Semi-aromatic polyamide (SAP)/spherical mesoporous silica nanocomposite reverse osmosis membrane (MSS RO)	Interfacial polymerization (IP)	SEM-FTIR, Zeta potential, transmission electron microscopy (TEM), pore diameter (D)	63–73	94–96	2,000 mg/L NaCl aqueous solution with 25°C, and 1.5 MPa operating pressure.	[74]
Semi-aromatic polyamide (SAP)			40.3	97.54		
Full-aromatic polyamide (FAP)			25.6	98.33%		
PA/RO membranes-MPC polymer-grafted membranes	IP-grafting	FTIR, SEM	11.26	90:96	Aqueous 0.05 wt.% NaCl the feed. The flow rate and applied pressure were 9.9 mL/min and 0.75 MPa.	[35]
RO membrane	Commercial	Zeta potential	1.1–1.8 × 10⁻⁵ (m³/m² s) at 0.5:0.8 MPa	Arsenite As(III) rejection from 70%:96%	100 μg/L of feed As(III) concentration, 0.55 MPa transmembrane pressure for the NF membrane and 0.69 MPa transmembrane pressure for the RO membrane, a temperature of 20°C.	[75]
Polyamide nanofiltration			1.5–2.5 × 10⁻⁵ (m³/ m² s) 0.4:0.7 MPa	As(III) rejection 37%–80%		
PA/RO membrane	Interfacial polymerization (IP)	Infrared (ATR FTIR) spectroscopy, X-ray photoelectron spectroscopy (XPS), SEM, atomic force microscopy (AFM), contact angle (CA)	22–54	98–99	1.55 MPa using 2,000 ppm NaCl solution in cross-flow cells.	[76]

Table 7
Separation performances of polyamide nanofiltration (PA/NF) membrane

Membrane type	Preparation process	Characterization methods	Permeate flux (kg/m² h)	Salt rejection (%)	Operating condition	References
PA/NF membranes (SWC4, XLE, LE, ESPA3, NE90 and NF90)	Commercial fully aromatic PA membrane, interfacial polymerization	Atomic force microscopy, transmission electron microscopy, contact angle measurement, streaming potential analysis	54–163	90%–97%	10 mM NaCl solution at pH 7. The applied pressure was 1,380 kPa (200 psi = 13.6 bar).	[77]
Thin-film composite PA membranes NF membranes (NFT-50, NF200, NF90 and Desal-5DK)	Commercial aromatic PA membrane	Flow rate and permeability	53	40–95	Feed solution of KCl (20 mM) 60°C at 6 bar membrane area 0.36 m².	[78]
NF200 membrane (Dow FILMTEC)	Commercial	FTIR	71	97 20	Aqueous (MgSO₄) 100 ppm feed solution aniline	[79]
Polyamide NF membranes				50–90 NaCl 70–90 CaCl₂	aqueous solutions NaCl–water (1–50 mol/m³, pH 3–6.5) and CaCl₂–water (1–500 mol/m³, pH 5.3–6.5) solutions at room temperature at 25°C, 20–25 bar.	[80]
TFC PANF membrane, AFC80	Commercial aromatic polyamide	The membrane surface charge was estimated by performing the electrokinetic characterization of the membrane.	15–75	98–99.5	Lead nitrate solutions with 50 to 300 mg Pb/L (at pH 5.7 and temperature of 25°C.	[81]

Table 8
Three case case studies of polyamide membrane applications in reverse osmosis of seawater, water treatment and industrial pilot plant

Case	Case 1	Case 2	Case 3
Paper title and reference	Seawater RO: Minera Esperanza, Chile [87,88]	RO water treatment system: Village of Tequesta, USA [87,88]	NFPA for rejection of Pb(II) in aqueous solutions at industrial pilot plant [89]
Membrane type	Polyamide RO-TFC-SW MegaMagnum SW: Spiral wound Manufacture: Koch Membranes, Lenntech	Polyamide RO-TFC-HR MegaMagnum SW: Spiral wound Manufacture: Koch Membranes, Lenntech	Nanofiltration (NF) polyamide commercial membranes TFC-AFCS0PCI
Project details	Location: Michilla Port, Chile, Desalination Capacity: 80 m³/h	Location: Village of Tequesta, Palm Beach County, Florida Capacity: 19,303 m³/d	Industrial pilot plant designed by the IPFM Research Group, University of Cantabria, Spain
Problem	Minera Esperanza's copper-gold mine is about 1,500 km north of Chile's capital city of Santiago. As a result of being at a desert area there is a big shortage of drinking water and being far from sources of potable water as the closest cities are from 50 to 70 km away which make it not logical to ship high amount of water by truck, seawater was the only accepted source of water.	Village of Tequesta depends on aquifer water as main source for water supply. Main problem was that salt water overlap with the superficial aquifer so that it is needed to apply desalination system. Aeration filtration system had been applied to the upper aquifer to remove iron then water would be chlorinated, but this treatment would be effective only for the upper aquifer, which was much purer than deeper water that actually needs desalination.	Lead could be considered as one of the most important pollutants that affect health badly even at low ratios. In order to that, it is essential to remove lead ions from both industrial and municipal water. Actually, NF membranes would highly remove lead ions efficiently as NF, which has the advantage of combining size and electrical effects [90].
Challenge	To apply an effective way with low cost as much as possible to provide potable water to mining camps in remote areas (RO system).	Supply a desalination system that would be able to cover the village residents needs of treated water.	Analyze the effect of using of NFPA membranes to remove lead ions from wastewater.
Solution	As result of lack of surface or ground water, solution was to make use of seawater by using membrane technology. Koch Membrane Systems (KMS) was selected to develop seawater reverse osmosis (RO) system. MegaMagnum® had been used for this purpose. Main feature was being of high capacity, made from a unique thin-film composite developed specifically for seawater applications. In addition, MegaMagnum seawater elements have reduced footprint, costing, and installation time. As result of large diameter, RO systems use one-seventh the number of elements compared to standard 8-inch elements and contain fewer o-ring seals, which prevent mixing between the seawater and product water.	Reverse osmosis (RO) is the most effective method to removing dissolved salts from water. Koch Membrane Systems (KMS) (was selected to supply the required desalination system) by Arcadis Engineering, the firm that had designed the water treatment plant for the Village of Tequesta. The system would be constructed of three RO streams each of 1.2 mg d (4,542 m³/d) with total capacity of 3.6 mg d (13,626 m³/d). Actually only two streams had been constructed. Results after applying the KMS membranes was so great as it had eliminated the need of maintenance to a very low percentage and so that labor cost had been reduced.	Industrial pilot plant designed and patented by the IPFM Research Group at the University of Cantabria to test the effect of using nanofiltration (NF) polyamide commercial membranes TFC-AFCS0PCI (thin-film composite) to remove lead ions. Actually the rejection tests were conducted with Pb(NO₃)₂. In order to allow the exchange of scale and its further industrial application, tests with aromatic polyamide commercial membrane TFC-AFC80PCI were made in the industrial pilot plant.

(Continued)

Table 8 Continued

Case	Case 1	Case 2	Case 3
Treatment plant system	Seawater drawn from the Pacific Ocean is the source of water supplied to the copper-gold mine. The seawater is pumped for about a mile to a water treatment unit that includes a pre-filtration system, then water is pumped to the RO system which consists of two skids, each consists of two MegaMagnum® RO vessels including an effective membrane surface area of 2,833 m² (equivalent to 76 standard size 8″ × 40″ elements). Permeate is disinfected using chlorine in order to make it suitable for drinking water. The permeate capacity is 1,968 m³/d with feed of total dissolved solids (TDS) of 40,000 ppm.	The RO system was designed as a concrete block structure in the architectural landscape of the village. Proper pumps are used to pump water from deeper water source, and then feed pumps are used to pump water to the pre-treatment stage, which includes dosing of sulphuric acid to lower the water pH to keep the hydrogen sulfide gas dissolved in the well water throughout the process. An anti-scalant is then added to prevent the precipitation of carbonates then water is passed through microfiltration step then go to high pressure pump so as to apply the suitable feed pressure to the RO membranes. Mainly required high pressure is about 276 psi (20 bar) as water is applied to the semi-permeable membranes to separate the impurities, the concentrate is discharged and the permeate from the RO is pumped to a treated water tank, where it's mixed with 10,219 m³/d water had been drawn from the upper aquifer and go to a filtered system, the entire mix is then treated through the standard aeration filtration process, after that water mixture goes into a clear well. The treated water after that is chlorinated. The RO permeate is like a distilled water, which makes it of higher quality than the older water source. As the older source (water from upper aquifer) comes out with a couple hundred parts per million of calcium hardness, which improves the taste. By blending it with the newer source (RO desalination system) there is still sufficient calcium for taste concerns but overall it's a purer end product also with capacity of 19,303 m³/d of total which covers residents needs even in times of peak demand.	Treatment system operating conditions were as following: pressures up to 4MP, feed flow in the range of 400–1,000 L/h, temperatures of (25°C–40°C). The results showed the high efficiency of NF process for the removal of Pb(II), with a high rejection, R, 80%–94%, for a feed concentration from 1–120 ppm. operating conditions such as temperature, pressure, permeate flux or feed salt concentration demonstrates the influence on the rejection of Pb(II) ions. In case of low concentration of Pb(II) at the permeate, actually (among 0.06 and 9 ppm respectively), so that water would be of good quality so as to be reused again.
Main conclusion or recommendation	Seawater desalination using polyamide RO membrane is efficient and dependable.	Water treatment system via PA membrane able to cover the needed of treated water for residents.	PA membranes are capable to separate metal such as lead ions from wastewater.

membrane morphology, leads to improved membrane separation efficiency and decreasing permeate flux [24,85].

4.3.3. Artificial neural network models based on quantitative structure–activity relationship for predicting rejection

Yangali-Quintanilla et al. [86] developed an artificial neural network (ANN) model that depended on quantitative structure–activity relationship for determining separation factor of neutral organic compounds by PA/NF and RO membranes. They concluded that salt rejection in combination with solute properties can be applied to predict organic solute rejection by the membrane. Intended for the mainly capable ANN models, the self-determining predicted separation values were compared to measured separation and a good relation was established.

5. Case studies of applications of polyamide membranes in reverse osmosis of seawater and urban water treatment and in an industrial pilot plant

Comprehensive reviews of three case studies in the application of polyamide membrane are summarized in Table 8. For example, Case 1 reported seawater desalination via polyamide RO membrane at Minera Esperanza, Chile [87], while Case 2 indicated polyamide RO membrane for a water treatment system at Village of Tequesta, USA [88], whereas Case 3 presented rejection of Pb(II) in aqueous solutions at industrial pilot plant using nanofiltration (NF) polyamide commercial membranes TFC [89]. All three examples demonstrated the wide successful application of polyamide membranes at a commercial scale.

6. Conclusions

Polyamide (PA) membranes can be successfully prepared via phase inversion process, interfacial polymerization (IP) and electro- spinning. Nevertheless, the electro-spinning process appears to be constrained by very slow rates of fiber production. Mathematical models have been developed to better describe and understand the behavior of PA/polymer 2/solvent membrane formation by the phase inversion process. The effect of polyamide composition on the change of Gibbs free energy was always negative and the mixing of polymer solution was stable for all the polymers compositions at room temperature. In addition, the surface properties (roughness, surface charge, hydrophilicity) and bulk properties (permeation rate, separation) have been measured to be mostly inter-dependent, as all those were determined by the polyamide chemistry and any associated surface coating layer.

Diffusion models for polyamide membranes have been utilized to study the effects of immersion/precipitation time in the coagulation bath and on the polymer blend formation. The model results indicated that the solvent was segregating from polymer solution and dissolving in the coagulation bath during precipitation time. The volume fraction of solvent increased in the bath and the volume fraction of polymer decreased because of the membrane formation. The models predicted the formation of a uniform membrane for all compositions with membrane thickness.

While polyamide reverse osmosis membranes have been widely applied in water treatment such as desalination, a need still exists for improved characterization of the transport behavior of polyamide membranes during reverse osmosis conditions. Additional improvements are also essential for phase inversion and interfacial polymerization. It is recommended that the less utilized membrane preparation techniques such as electro-spinning and track-etching be investigated further to enhance their application in large-scale desalination. One can speculate that this may result in more economically produced drinking water being readily available globally to millions of individuals. The enhanced understanding of the extraordinary capabilities exhibited by these polymeric films, is critical for further improvement and utilization of the technology.

References

[1] L.E. Peng, Z. Yang, L. Long, S. Zhou, H. Guo, C.Y. Tang, A critical review on porous substrates of TFC polyamide membranes: mechanisms, membrane performances, and future perspectives, J. Membr. Sci., 641 (2022) 119871, doi: 10.1016/j.memsci.2021.119871.

[2] H. Sanaeepur, A.E. Amooghin, M.M.A. Shirazi, M. Pishnamazi, S. Shirazian, Water desalination and ion removal using mixed matrix electrospun nanofibrous membranes: a critical review, Desalination, 521 (2022) 115350, doi: 10.1016/j.desal.2021.115350.

[3] M. Ohno, C. Manalo, L. Rossetto, T. Okuda, S. Nakai, W. Nishijima, Effect of coexisting metal ions on the degradation of polyamide reverse osmosis membrane by hypochlorite treatment, Desalination, 381 (2016) 126–134.

[4] J. Wang, W. Zhao, B. Wang, G. Pei, C. Li, Multilevel-layer-structured polyamide-6/poly(trimethylene terephthalate) nanofibrous membranes for low-pressure air filtration, J. Appl. Polym. Sci., 134 (2017) 44716, doi: 10.1002/app.44716.

[5] L. Ahmadian-Alam, M. Kheirmand, H. Mahdavi, Preparation, characterization and properties of PVDF-g-PAMPS/PMMA-*co*-PAMPS/silica nanoparticle as a new proton exchange nanocomposite membrane, Chem. Eng. J., 284 (2016) 1035–1048.

[6] Z. Zhou, S. Rajabzadeh, A.R. Shaikh, Y. Kakihana, T. Ishigami, R. Sano, H. Matsuyama, Preparation and characterization of antifouling poly(vinyl chloride-*co*-poly(ethylene glycol)methyl ether methacrylate) membranes, J. Membr. Sci., 498 (2016) 414–422.

[7] S. Xu, H. Lin, G. Li, J. Wang, Q. Han, F. Liu, Anionic covalent organic framework as an interlayer to fabricate negatively charged polyamide composite nanofiltration membrane featuring ions sieving, Chem. Eng. J., 427 (2022) 132009, doi: 10.1016/j.cej.2021.132009.

[8] S. Habib, S.T. Weinman, A review on the synthesis of fully aromatic polyamide reverse osmosis membranes, Desalination, 502 (2021) 114939, doi: 10.1016/j.desal.2021.114939.

[9] M.Q. Seah, W.J. Lau, P.S. Goh, H.-H. Seng, R.A. Wahab, A.F. Ismail, Progress of interfacial polymerization techniques for polyamide thin film (nano)composite membrane fabrication: a comprehensive review, Polymers, 12 (2020) 2817, doi: 10.3390/polym12122817.

[10] M. Dalwani, N.E. Benes, G. Bargeman, D. Stamatialis, M. Wessling, Effect of pH on the performance of polyamide/polyacrylonitrile based thin-film composite membranes, J. Membr. Sci., 372 (2011) 228–238.

[11] R. Bernstein, S. Belfer, V. Freger, Bacterial attachment to RO membranes surface-modified by concentration-polarization-enhanced graft polymerization, Environ. Sci. Technol., 45 (2011) 5973–5980.

[12] A.K. Holda, B. Aernouts, W. Saeys, I.F.J. Vankelecom, Study of polymer concentration and evaporation time as phase inversion parameters for polysulfone-based SRNF membranes, J. Membr. Sci., 442 (2013) 196–205.

[13] A. Cano-Odena, M. Spilliers, T. Dedroog, K. De Grave, J. Ramon, I.F.J. Vankelecom, Optimization of cellulose acetate nanofiltration membranes for micropollutant removal via genetic algorithms and high throughput experimentation, J. Membr. Sci., 366 (2011) 25–32.

[14] L. Lin, R. Lopez, G.Z. Ramon, O. Coronel, investigating the void structure of the polyamide active layers of thin-film composite membranes, J. Membr. Sci., 497 (2016) 365–376.

[15] S. Hermans, R. Bernstein, A. Volodin, I.F.J. Vankelecom, Study of synthesis parameters and active layer morphology of interfacially polymerized polyamide–polysulfone membranes, React. Funct. Polym., 86 (2015) 199–208.

[16] G.Z. Ramon, E.M.V. Hoek, Transport through composite membranes, part 2: impacts of roughness on permeability and fouling, J. Membr. Sci., 425–426 (2013) 141–148.

[17] W.J. Lau, A.F. Ismail, N. Misdan, M.A. Kassim, A recent progress in thin-film composite membrane: a review, Desalination, 287 (2012) 190–199.

[18] P.J. Flory, Principles of Polymer Chemistry, Cornell University Press, Ithaca, NY, 1969.

[19] http://www.kochmembrane.com/Learning-Center/Water-Wastewater, Filtration/Characteristics-of-Membrane-Products.aspx

[20] A.K. Ghosh, B.H. Jeong, X. Huang, E.M.V. Hoek, Impacts of reaction and curing conditions on polyamide composite reverse osmosis membrane properties, J. Membr. Sci., 311 (2008) 34–45.

[21] M.N. Mahboub, M. Pakizeha, S. Davari, Preparation and characterization of UZM-5/polyamide thin film nanocomposite membrane for dewaxing solvent recovery, J. Membr. Sci., 459 (2014) 22–32.

[22] J. Zhang, Y. Zhang, H. Zhang, J. Dang, J. Liu, Preparation and characterization of a novel polyamide charged mosaic membrane, Chin. J. Chem. Eng., 18 (2010) 569–576.

[23] A. Alkhudhiri, N. Darwish, N. Hilal, Membrane distillation: a comprehensive review, Desalination, 287 (2012) 2–18.

[24] E. Drioli, L. Giorno, Membrane Operations: Innovative Separations and Transformations, Wiley-VCH, Germany, ISBN: 978-3-527-32038-7, 2009. Available at: https://onlinelibrary.wiley.com/doi/pdf/10.1002/9783527626779

[25] A. EL-Gendi, Ternary Phase Diagram Construction and Membrane Morphology Evaluation, LAP Lambert Academic Publishing, Germany, ISBN: 978-3-659-57611-9, 2014.

[26] A. EL-Gendi, Phase Diagram and Membrane Desalination, Chapter 3 in Desalination Updates, ISBN: 978-953-51-2189-3, R.Y. Ning, Ed., Intech Open Limited, London, SW7 2QJ, United Kingdom, 2015. Available at: https://www.intechopen.com/chapters/48518

[27] A.T. El-Gendi, S.A. Ahmed, H.A. Talaat, Preparation and evaluation of flat membranes for phenols separation, Desalination, 206 (2007) 226–237.

[28] L.A. Nezam El-Din, A. El-Gendi, N. Ismail, K.A. Abed, A.I. Ahmed, Evaluation of cellulose acetate membrane with carbon nanotubes additives, J. Ind. Eng. Chem., 26 (2015) 259–264.

[29] W. Mark, The Guidebook to Membrane Desalination Technology, Balaban Desalination Publications, Italy, ISBN: 0-86689-065-3, 2007. Available at: http://www.desline.com/WilfBookIcomplete.pdf

[30] M. Mulder, Basic Principles of Membrane Technology, 2nd ed., Kluwer Academic, Springer, Dordrecht, Boston, London, ISBN: 0-7923-4248-8, 1996. Available at: file:///C:/Users/ecs/Downloads/Mulder1996_Book_BasicPrinciplesOfMembraneTechn.pdf

[31] S.L. Duraikkannu, R. Castro-Muñoz, A. Figoli, A review on phase inversion technique-based polymer microsphere fabrication, Colloid Interface Sci. Commun., 40 (2021) 100329, doi: 10.1016/j.colcom.2020.100329.

[32] M.C. Porter, Handbook of Industrial Membrane Technology, Noyes Publications, Park Ridge, New Jersey, U.S.A., 1990, pp. 61–70.

[33] R.W. Baker, Membrane Technology and Applications, 2nd ed., John Wiley & Sons, Ltd., West Sussex PO19 8SQ, England, ISBN: 0-470-85445-6, 2004. Available at: http://aulanni.lecture.ub.ac.id/files/2012/01/MembraneTechnologyApplication1.pdf

[34] Y.-L. Liu, C.-H. Yu, J.-Y. Lai, Poly(tetrafluoroethylene)/polyamide thin-film composite membranes via interfacial polymerization for pervaporation dehydration on an isopropanol aqueous solution, J. Membr. Sci., 315 (2008) 106–115.

[35] https://en.wikipedia.org/wiki/Thin-film_composite_membrane

[36] R. Dai, J. Li, Z. Wang, Constructing interlayer to tailor structure and performance of thin-film composite polyamide membranes: a review, Adv. Colloid Interface Sci., 282 (2020) 102204, doi: 10.1016/j.cis.2020.102204.

[37] G.D. Kang, M. Liu, B. Lin, Y.M. Cao, Q. Yuan, A novel method of surface modification on thin-film composite reverse osmosis membrane by grafting poly(ethylene glycol), Polymer, 48 (2007) 1165–1170.

[38] D. Saeki, S. Nagao, I. Sawada, Y. Ohmukai, T. Maruyama, H. Matsuyama, Development of antibacterial polyamide reverse osmosis membrane modified with a covalently immobilized enzyme, J. Membr. Sci., 428 (2013) 403–409.

[39] B. Khorshidi, T. Thundat, B.A. Fleck, M. Sadrzadeh, Thin-film composite polyamide membranes: parametric study on the influence of synthesis conditions, RSC Adv., 5 (2015) 54985–54997.

[40] D. Rana, T. Matsuura, Surface modifications for antifouling membranes, Chem. Rev., 110 (2010) 2448–2471.

[41] S. Yu, M. Liu, X. Liu, C. Gao, Performance enhancement in interfacially synthesized thin-film composite polyamide–urethane reverse osmosis membrane for seawater desalination, J. Membr. Sci., 342 (2009) 313–320.

[42] M. Fathizadeh, A. Aroujalian, A. Raisi, Effect of lag time in interfacial polymerization on polyamide composite membrane with different hydrophilic sub layers, Desalination, 284 (2012) 32–41.

[43] J. Gilron, S. Belfer, P. Vaisanen, M. Nystrom, Effects of surface modification on antifouling and performance properties of reverse osmosis membranes, Desalination, 140 (2001) 167–179.

[44] M. Liu, S. Yu, J. Tao, C. Gao, Preparation, structure characteristics and separation properties of thin-film composite polyamide-urethane seawater reverse osmosis membrane, J. Membr. Sci., 325 (2008) 947–956.

[45] C. Klaysom, S. Hermans, A. Gahlaut, S. Van Craenenbroeck, I.F.J. Vankelecom, Polyamide/polyacrylonitrile (PA/PAN) thin-film composite osmosis membranes: film optimization, characterization and performance evaluation, J. Membr. Sci., 445 (2013) 25–33.

[46] A. Ismail, L. Yean, Review on the development of defect-free and ultrathin-skinned asymmetric membranes for gas separation through manipulation of phase inversion and rheological factors, J. Appl. Polym. Sci., 88 (2003) 442–451.

[47] A. El-Gendi, S.S. Ali, S.A. Ahmed, H.A. Talaat, Development of membrane blend using casting technique for water desalination, Membr. Water Treat., 3 (2012) 185–200.

[48] A. Rawajefa, Polyamide based composite membrane, part 1: preparation and characterization, Desalination, 179 (2005) 265–272.

[49] A.A. Lefebvre, J.H. Lee, N.P. Balsara, B. Hammouda, Fluctuations in highly metastable polymer blends, J. Polym. Sci., Part B: Polym. Phys., 38 (2000) 1926–1930.

[50] A. El-Gendi, A. Amin, H. Abdallah, Mathematical model for polyamide-6/chitosan blend membrane preparation, Res. J. Pharm., Biol. Chem. Sci. RJPBCS, 7 (2016) 892–906.

[51] A. El-Gendi, H. Abdallah, Thermodynamic modeling of polyamide-6 (PA-6)/cellulose acetate (CA) blend membrane prepared via casting technique, J. Polym. Eng., 8 (2013) 701–712.

[52] F. Pacheco, R. Sougrat, M. Reinhard, J.O. Leckie, I. Pinnau, 3D visualization of the internal nanostructure of polyamide thin films in RO membranes, J. Membr. Sci., 501 (2016) 33–44.

[53] D.J. Lin, L.P. Cheng, S.P. Lin, Effect of compatible nucleation seeds on the morphology of porous Nylon-6 membrane, Desalination, 145 (2002) 31–37.

[54] M. Zeni, R. Riveros, J.F. de Souza, K. Mello, C. Meireles, G.R. Filho, Morphologic analysis of porous polyamide 6,6 membranes prepared by phase inversion, Desalination, 221 (2008) 294–297.

[55] A.M.W. Bulte, M.H.V. Mulder, C.A. Smolders, H. Strathmann, Induced phase separation with crystallizable nylons. II. Relation to final membrane morphology, J. Membr. Sci., 121 (1996) 51–58.

[56] D.J. Lin, C.L. Chang, C.K. Lee, L.P. Cheng, Fine structure and crystallinity of porous nylon-66 membranes prepared by phase inversion in the water/formic acid/Nylon 66 system, Eur. Polym. J., 42 (2006) 356–367.

[57] A.M.W. Bulte, M.H.V. Mulder, C.A. Smolders, H. Strathmann, Diffusion induced phase separation with crystallizable nylons. I. Mass transfer processes for nylon 4,6, J. Membr. Sci., 121 (1996) 37–49.

[58] J. Yin, G. Zhu, B. Deng, Graphene oxide (GO) enhanced polyamide (PA) thin-film nanocomposite (TFN) membrane for water purification, Desalination, 379 (2016) 93–101.

[59] M. Moslehi, H. Mahdavi, A. Ghaffari, Preparation and characterization of polyamide thin-film composite nanofiltration membrane based on polyurethane nanofibrous support, J. Polym. Environ., 29 (2021) 2463–2477.

[60] A.M. Kadhom, M.H. Al-Furaiji, Z.N. Abudi, Evaluation of thin-film composite forward osmosis membranes: effect of polyamide preparation conditions, Drinking Water Eng. Sci., 14 (2021) 45–52.

[61] A. Rahimpour, M. Jahanshahi, N. Mortazavian, S.S. Madaeni, Y. Mansourpanah, Preparation and characterization of asymmetric polyethersulfone and thin-film composite polyamide nanofiltration membranes for water softening, Appl. Surf. Sci., 256 (2010) 1657–1663.

[62] X. Li, C. Zhang, S. Zhang, J. Li, B. He, Z. Cui, Preparation and characterization of positively charged polyamide composite nanofiltration hollow fiber membrane for lithium and magnesium separation, Desalination, 369 (2015) 26–36.

[63] S.K. Jewrajka, A.V.R. Reddy, H.H. Rana, S. Mandal, S. Khullar, S. Haldar, N. Joshi, P.K. Ghosh, Use of 2,4,6-pyridinetricarboxylic acid chloride as a novel co-monomer for the preparation of thin-film composite polyamide membrane with improved bacterial resistance, J. Membr. Sci., 439 (2013) 87–95.

[64] A. Linggawati, A.W. Mohammad, C.P. Leo, Effects of APTEOS content and electron beam irradiation on physical and separation properties of hybrid nylon-66 membranes, Mater. Chem. Phys., 133 (2012) 110–117.

[65] A. El-Gendi, S. Ali, H. Abdalla, M. Saied, Microfiltration/ultrafiltration polyamide-6 membranes for copper removal from aqueous solutions, Membr. Water Treat., 7 (2016) 55–70.

[66] H.H. Chang, S.C. Chen, D. Lin, L.-P. Cheng, Preparation of bi-continuous nylon-66 porous membranes by coagulation of incipient dopes in soft non-solvent baths, Desalination, 313 (2013) 77–86.

[67] M. Yanilmaz, M. Dirican, X. Zhang, Evaluation of electrospun SiO$_2$/nylon 6,6 nanofiber membranes as a thermally-stable separator for lithium-ion batteries, Electrochim. Acta, 133 (2014) 501–508.

[68] J.T. Jung, H.H. Wang, J.F. Kim, S.M. Jeon, S.H. Park, W.H. Lee, S.J. Moon, E. Drioli, Y.M. Lee, Microfiber aligned hollow fiber membranes from immiscible polymer solutions by phase inversion, J. Membr. Sci., 617 (2021) 118654, doi: 10.1016/j.memsci.2020.118654.

[69] G.L. Jadav, P.S. Singh, Synthesis of novel silica-polyamide nanocomposite membrane with enhanced properties, J. Membr. Sci., 328 (2009) 257–267.

[70] K. Košutić, L. Kaštelan-Kunst, B. Kunst, Porosity of some commercial reverse osmosis and nanofiltration polyamide thin-film composite membranes, J. Membr. Sci., 168 (2000) 101–108.

[71] V. Kolev, V. Freger, Hydration, porosity and water dynamics in the polyamide layer of reverse osmosis membranes: a molecular dynamics study, Polymer, 55 (2014) 1420–1426.

[72] O.A. Hommaid, I.M. Al Bakri, Preparation of polyamide-6/zeolite-Y hybrid membranes, and the evaluation of their structural, physical and mechanical properties, Egypt. J. Chem., 63 (2020) 4625–4633.

[73] Q. Zhang, C. Zhang, J. Xu, Y. Nie, S. Li, S. Zhang, Effect of poly(vinyl alcohol) coating process conditions on the properties and performance of polyamide reverse osmosis membranes, Desalination, 379 (2016) 42–52.

[74] Q. Li, H. Yu, F. Wu, J. Song, X. Pan, M. Zhang, Fabrication of semi-aromatic polyamide/spherical mesoporous silica nanocomposite reverse osmosis membrane with superior permeability, Appl. Surf. Sci., 363 (2016) 338–345.

[75] F. Chang, W. Liu, X. Wang, Comparison of polyamide nanofiltration and low-pressure reverse osmosis membranes on As(III) rejection under various operational conditions, Desalination, 334 (2014) 10–16.

[76] T. Wang, L. Dai, Q. Zhang, A. Li, S. Zhang, Effects of acyl chloride monomer functionality on the properties of polyamide reverse osmosis (RO) membrane, J. Membr. Sci., 440 (2013) 48–57.

[77] C.Y. Tang, Y.N. Kwon, J.O. Leckie, Effect of membrane chemistry and coating layer on physiochemical properties of thin-film composite polyamide RO and NF membranes II. Membrane physiochemical properties and their dependence on polyamide and coating layers, Desalination, 242 (2009) 168–182.

[78] M. Nilsson, G. Tragardha K. Ostergren, Influence of temperature and cleaning on aromatic and semi-aromatic polyamide thin-film composite NF and RO membranes, Sep. Purif. Technol., 62 (2008) 717–726.

[79] A.B. David, S. Bason, J. Jopp, Y. Oren, Partitioning of organic solutes between water and polyamide layer of RO and NF membranes: correlation to rejection, J. Membr. Sci., 281 (2006) 480–490.

[80] C. Mazzoni, S. Bandini, The role of the electrolyte on polyamide NF membranes performances: experimental analysis with NaCl and CaCl$_2$ solutions, Desalination, 200 (2006) 135–137.

[81] C.V. Gherasim, J. Cuhorka, P. Mikulasek, Analysis of lead(II) retention from single salt and binary aqueous solutions by a polyamide nanofiltration membrane: experimental results and modeling, J. Membr. Sci., 436 (2013) 132–144.

[82] A.K. Ghosh, R.C. Bindal, S. Prabhakar, P.K. Tewari, Composite polyamide reverse osmosis (RO) membranes – recent developments and future directions, Mater. Phys., 321 (2011) 43.

[83] J. Hosch, E. Staude, Preparation and investigation of chemically modified porous polyamide ultrafiltration membranes, J. Membr. Sci., 121 (1996) 71–82.

[84] M. Manttari, A. Pihlajamaki, E. Kaipainen, M. Nystrom, Effect of temperature and membrane pre-treatment by pressure on the filtration properties of nanofiltration membranes, Desalination, 145 (2002) 81–86.

[85] R.A. Knight, T. Hazlett, C.C. Gryte, Effect of high temperature annealing on the capillarity of polyamide microporous membranes, Stud. Polym. Sci., 11 (1992) 299–313.

[86] V. Yangali-Quintanilla, A. Verliefde, T.-U. Kim, A. Sadmani, M. Kennedy, G. Amy, Artificial neural network models based on QSAR for predicting rejection of neutral organic compounds by polyamide nanofiltration and reverse osmosis membranes, J. Membr. Sci., 342 (2009) 251–262.

[87] https://www.kochseparation.com/resources/case-studies/

[88] https://www.lenntech.com/products/membrane/romembranes.htm

[89] J.A. Otero, A. Otero-Fernandez, M.D. Fernandez, L. Palacio, P. Pradanos, Use of nanofiltration aromatic polyamide membranes. Case study: influence of operating conditions on the rejection of Pb(II) in aqueous solutions at industrial pilot plant, Procedia Eng., 44 (2012) 2023–2025.

[90] X. Feng, D. Liu, H. Ye, D. Peng, J. Wang, S. Han, Y. Zhang, High-flux polyamide membrane with improved chlorine resistance for efficient dye/salt separation based on a new N-rich amine monomer, Sep. Purif. Technol., 278 (2021) 119533, doi: 10.1016/j.seppur.2021.119533.